

# Circulating Tumor Cells Are Transcriptionally Similar to the Primary Tumor in a Murine Prostate Model

Kimberly T. Helzer,<sup>1</sup> Helen E. Barnes,<sup>1</sup> Laura Day,<sup>1</sup> Jeanne Harvey,<sup>2</sup> Paul R. Billings,<sup>2</sup> and Allyn Forsyth<sup>1</sup>

<sup>1</sup>Cx Biosystems, La Jolla, California and <sup>2</sup>CELlective Dx, Mountain View, California

## Abstract

**The abundance of circulating tumor cells (CTC) indicates patient prognosis. Molecular characterization of CTCs may add additional information about a patient's disease. However, currently available methods are limited by contamination with blood cells. We describe a study using a modified CTC-chip to capture CTCs from an orthotopic xenograft model. Using laser capture microscopy to collect CTCs from the chip, we compared transcripts from purified CTCs with those from primary and metastatic tissue. Transcriptional profiles showed strong concordance among primary, metastatic, and CTC sources. Moreover, cells captured on the chip were viable and could be expanded in culture. We conclude that the CTC-chip is a useful tool to further characterize animal models of cancer and that viable CTCs can be isolated and show transcriptional similarity to solid tumors.** [Cancer Res 2009;69(19):7860–6]

## Introduction

Circulating tumor cells (CTC) are thought to be released into the bloodstream from tumors of epithelial origin (1). Recently, the number of CTCs has been shown to predict patient outcome for metastatic breast, metastatic colorectal, and metastatic prostate cancer (2, 3). In addition to indicating patient prognosis, it may be possible to use isolated CTCs to interrogate the current biology of a patient's cancer (4).

A lack of consensus on how similar CTCs are to parent tumors currently precludes their use as a surrogate for solid tumor biopsies. Published reports of genetic mutations (4) and mRNA profiles (5) used enriched CTCs in a background of leukocytes. These studies were somewhat limited by the use of enriched, not purified, CTC molecular templates, as signal from nontarget cells can overwhelm molecular signatures from the rare CTCs.

Recent publications suggest that certain xenograft models generate CTCs. In particular, specific reports of prostate cancer cells implanted into the prostate of immune compromised mice resulted not only in tumor formation but also in metastases and the generation of viable CTCs (5, 6). A similar study surveyed breast cancer cell lines and reported one model from which CTCs were observed (6).

Using a plastic version of the previously described CTC-chip, we showed isolation and analysis of CTCs from a xenograft model of prostate cancer. Cells captured on the CTC-chip are viable and can be expanded in culture. Using a laser pressure catapulting (LPC) procedure, we showed that CTCs can be isolated away from contaminating blood cells and that purified CTC populations were similar to primary tumor and tested metastatic sites within the dynamic range of measured transcripts.

## Materials and Methods

**Cell lines and orthotopic mouse model.** PC-3 cells (American Type Culture Collection) were grown in RPMI 1640 supplemented with 10% fetal bovine serum (FBS) and penicillin-streptomycin (Invitrogen).

The orthotopic model has been previously described (7, 8). Cardiac blood (0.20–1.0 mL) was collected on sacrifice in EDTA tubes (BD Biosciences) and stored at room temperature up to 2 h until processed. Whole-body and open cavity imaging was performed as previously described (7). Primary and metastatic tumors were discriminated from adjacent normal tissue via their green fluorescent protein (GFP) fluorescence, selectively isolated, and flash frozen in liquid nitrogen. RNA from tissue was isolated using the RNeasy Plus RNA kit (Qiagen).

For expansion of captured CTCs, mouse blood was run across a CTC-chip and washed as described below. The tape was removed from the chip and placed in a dish of RPMI 1640/10% FBS/penicillin-streptomycin under 5.0% CO<sub>2</sub> and grown for 12 d. Cells were imaged by fluorescence microscopy and phase-contrast microscopy.

**Histochemical analysis.** For histochemical analysis, dried blood smears or cultured CTCs were fixed for 1 min in 100% methanol (Sigma) and stained with Wright-Giemsa stain (Sigma) per the manufacturer's protocol. For bright-field immunohistochemical analysis, the Vectastain Elite avidin-biotin complex kit and 3,3'-diaminobenzidine (DAB) substrate kit for peroxidase (Vector Laboratories) were used. Reagents were flowed through the CTC-chip at 50  $\mu$ L/min. Cells captured on the chip were fixed with 4% paraformaldehyde, permeabilized with 0.2% Triton X-100 (Sigma), and blocked with normal goat serum. Mouse anti-cytokeratin monoclonal antibody (clone AE1/AE3; Invitrogen) was used at a 1:200 concentration followed by biotin-labeled anti-mouse IgG, horseradish peroxidase-labeled avidin, and then DAB.

**Preparation of CTC capture chip.** The design and conjugation of antibodies to a CTC-chip has been described previously (9) with the following modifications. The chips were made from plastic using an embossing process. Chips were cleaned and activated with oxygen plasma, incubated with 4% 11-(succinimidyl)undecyldimethylethoxysilane (Gel-est) in ethanol, washed with ethanol, incubated with 10  $\mu$ g/mL NeutrAvidin (Pierce), washed with PBS (Cellgro), and then incubated with 10  $\mu$ g/mL of biotinylated goat anti-EpCAM antibody (R&D Systems). Stability was extended by washing the antibody-coated chips in a sugar buffer composed of 2 mmol/L L-histidine and 60 mmol/L trehalose (Sigma). Chips were then sealed with adhesive tape and Tygon tubing attached to ports. Chips were stored desiccated at 4°C until use (up to 1 mo).

**CTC capture, imaging, and enumeration on the CTC-chip.** Sealed chips were attached via 2-Stop PharMed BPT tubing (Cole-Parmer) to IPC peristaltic pumps (Ismatec), which allowed simultaneous runs of four samples per pump. Chips were placed on elevated level platforms and

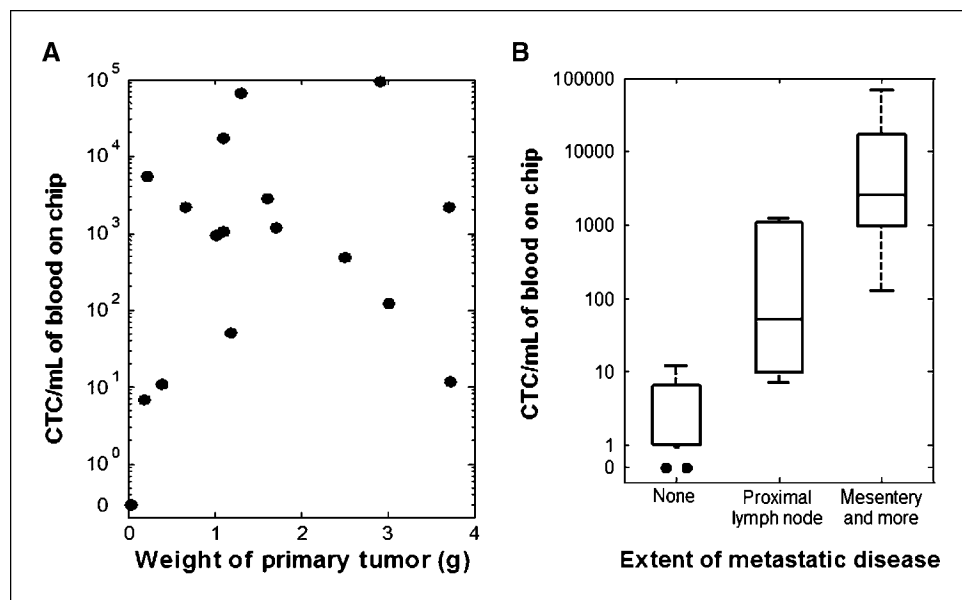
**Note:** Supplementary data for this article are available at Cancer Research Online (<http://cancerres.aacrjournals.org/>).

K.T. Helzer and H. E. Barnes contributed equally to this work.  
CELlective Dx is now On-Q-ity.

**Requests for reprints:** Jeanne Harvey, On-Q-ity, 610 Lincoln St., Waltham, MA 02451. Phone: 781-895-8100; Fax: 781-890-4636; E-mail: [jeanne.harvey@On-Q-ity.com](mailto:jeanne.harvey@On-Q-ity.com).

©2009 American Association for Cancer Research.  
doi:10.1158/0008-5472.CAN-09-0801

**Figure 1.** CTCs recovered from PC-3 tumor xenograft mice compared with (A) weight of primary tumor and (B) extent of metastatic disease. CTC number is plotted versus tumor weight in grams or the observed extent of metastasis from open cavity examination. B, box and whiskers plot representing animals with no detected metastasis ( $n = 3$ ; two represented by dots had no CTCs), dissemination to only the proximal lymph node ( $n = 4$ ), or dissemination to the mesentery and more ( $n = 10$ ).



primed with 1.0 mL of CAS buffer (Invitrogen). Blood was run at 16.7  $\mu\text{L}/\text{min}$  across the chip and washed with 1% bovine serum albumin (BSA)/PBS and Hoechst 33342 (Invitrogen) at a flow rate of 50.0  $\mu\text{L}/\text{min}$ . In some instances when transcriptional analysis was not to be performed, cells were fixed on the chip using 1% paraformaldehyde (EMS) and washed before imaging.

Samples used for transcriptional analysis were preprocessed. Specifically, blood samples were fixed by adding paraformaldehyde to a final concentration of 1% and incubating for 15 min at room temperature. An equal volume of 1% BSA/PBS/5 mmol/L EDTA was added followed by centrifugation at  $400 \times g$  for 2 min. Plasma and buffer were removed and blood was resuspended to the original volume with 1% BSA/PBS/5 mmol/L EDTA.

All chips were imaged on a BioView scanning microscope using a  $5\times$  objective. Events that were GFP and Hoechst positive were tagged by a BioView script as putative CTCs. Visual review of putative events was used for final enumeration of validated true CTCs as morphologically distinct GFP-positive cells with a Hoechst-stained nucleus.

**Validation of blood smear enumeration and calculation of CTC-chip capture efficiency.** PC-3 cells were stained with both CellTracker Green (Invitrogen) and Hoechst 33342 (Invitrogen). Cells were then fixed by adding paraformaldehyde to a final concentration of 1% and incubating for 15 min at room temperature. Stained cells were counted and added into 1 mL mouse blood. PC-3 cells were titrated to final concentrations of 10,000, 5,000 and 1,000 cells per mL of blood. For each titration, 10  $\mu\text{L}$  were pipetted onto slides in triplicate and scanned using a Leica DM fluorescent microscope. CellTracker Green-positive cells were counted using scanned images. Coincident Hoechst/CellTracker Green staining was also verified.

Having validated the accuracy of CTC enumeration using blood smears, we were able to show the efficiency of the CTC-chip by comparing CTCs captured on the chip with CTCs counted in blood smears. To enumerate CTCs in whole blood, 10  $\mu\text{L}$  of blood were spotted onto a glass slide with Hoechst 33342. Slides were scanned by BioView for CTC enumeration. CTC counts from the whole blood were then compared with counts from the same blood sample run over a CTC-chip.

**LPC collection of CTCs.** To isolate CTCs, preprocessed mouse blood was run across a CTC-chip as described above. Following enumeration, the tape was removed from the chip to allow fluid to evaporate. LPC protocols were modified from the manufacturer (Zeiss PALM MB IV) to use 72% power and a focal offset of a few microns to account for differences between the CTC-chip and a glass slide. LPC was used to collect 50 cells per chip in duplicate. Cells were captured in the lid of PALM microfuge tubes and immediately subjected to molecular analysis.

**Taqman assay development.** Numerous gene-specific intron-spanning Taqman assays were designed using the Human Universal ProbeLibrary

(UPL) Set and the UPL Assay Design software (Roche). The EGFR Taqman assay was purchased from Applied Biosystems (see Supplementary Data for sequences). A final panel of 42 gene-specific Taqman assays was selected based on individual and multiplex performance with template RNAs from various tissues or cell lines, as well as with PC-3 cells.

**RNA isolation and amplification from CTCs, tissues, and controls.** Control PC-3 RNA was isolated from tissue culture cells with the RNeasy Plus Mini kit (Qiagen). Samples of CTCs, PC-3 cells, 500 pg of tissue RNA, or 150 pg of control RNAs were collected and/or lysed with targeted cDNA preamplification via first-step reverse transcription-PCR (RT-PCR): 50  $^{\circ}\text{C}$  for 15 min, 95  $^{\circ}\text{C}$  for 2 min, and 18 cycles of 95  $^{\circ}\text{C}$  for 15 min, 60  $^{\circ}\text{C}$  for 4 min. cDNAs were generated with a 5  $\mu\text{L}$  master mix containing 0.05  $\mu\text{mol}/\text{L}$  primers (Integrated DNA Technologies) and 0.01  $\mu\text{mol}/\text{L}$  Taqman probes (Roche) from frozen aliquots, and 0.01  $\mu\text{L}$  SuperScript III RT/Platinum Taq mix (with RNaseOUT RNase inhibitor) and 1 $\times$  Reaction Buffer from the CellsDirect One-Step qRT-PCR kit (Invitrogen). Controls included prostate tissue RNA from a control non-tumor-bearing nude mouse, blood leukocyte RNA (UniChain Biosystems, Inc.), PC-3 RNA, and LPC or water negative controls. Preamplified cDNAs were routinely stored at  $-20^{\circ}\text{C}$  overnight and then diluted 1:5 with water for quantitative PCR (qPCR) analysis.

cDNAs were subjected to triplicate qPCR across the panel [42 genes with glyceraldehyde-3-phosphate dehydrogenase (*GAPDH*) and  $\beta$ -actin duplicated and 3 no-assay controls] using the standard BioMark Real-Time PCR protocol for 48.48 dynamic array chips (Fluidigm) with the following modification. Individual gene-specific Taqman assays containing 9.45  $\mu\text{mol}/\text{L}$  primers, 2.35  $\mu\text{mol}/\text{L}$  probes, and 0.5 $\times$  assay loading reagent were frozen in aliquots for use in qPCR.

**Taqman assay data analysis.** Statistical analysis was completed in Excel and Spotfire DecisionSite 9.1.1 for Microarray Analysis (Tibco Software, Inc.). Gene expression levels are reported as  $C_{t_{\text{norm}}}$  values following normalization of Ct values for each transcript to *GAPDH*. In cases where amplification was not detected during the 40-cycle qPCR, an arbitrary cycle number of Ct 50 was used for normalization purposes. Next,  $C_{t_{\text{norm}}}$  values from triplicate qPCRs were averaged, excluding any undetectable transcripts. Duplicate RT-PCRs were performed for all samples other than tissue. Respective  $C_{t_{\text{norm}}}$  values of duplicate RT-PCRs were subsequently averaged, excluding any undetectable transcripts. To examine correlations between tissues,  $C_{t_{\text{norm}}}$  values from respective RT-PCRs of primary tumor or lymph node metastatic tissue were averaged as a set. As we found  $C_{t_{\text{norm}}}$  values  $<15$  to be reproducible, we graphed only the 22 to 24 transcripts from our panel with these higher gene expression levels.

Multiple experimental data sets are presented in “heat map” format. In the process of generating the heat map, normalization between experiments was accomplished by autoscaling  $Ct_{norm}$  values within a single sample type, on a scale of 0 to 1, where 0 represents the lowest  $Ct_{norm}$  value and 1 represents undetected transcripts.

## Results

**Generation of CTCs in a model system.** To study CTC generation in a mouse model, we chose a model with cells that expressed GFP to monitor tumor growth and extent of disease using noninvasive whole-body imaging. Whole-body imaging and examination of the viscera after sacrifice allowed us to group the animals as having no metastatic spread from the primary tumor, spread only to adjacent lymph nodes, or disseminated into other organs of the body including the mesentery and, in some animals, to the diaphragm, liver, and pancreas. Necropsies did not include an analysis of the bones, so the full extent of metastases is not known, although metastatic spread in this model has been described in detail elsewhere (7) and included metastasis to the bones. Although the numbers of CTCs did not correlate with the weight of the primary tumor, there was a trend, although not statistically validated, toward greater CTCs with the extent of gross metastasis in the abdominal cavity (Fig. 1A and B). We attempted to obtain CTCs from peripheral site bleeds—foot pad, tail vein, and retro-orbital—as described elsewhere (6) and were likewise unable to consistently detect CTCs in these samples. Blood collected via terminal cardiac punctures generated an average of over 8 CTCs per  $\mu\text{L}$  across the 18 mice tested in this study.

**Measuring the efficiency of the CTC-chip.** The CTC-chip technology has been previously described and evaluated (9). To validate the ability of the CTC-chip to capture *in vivo* derived CTCs, we first showed the accuracy of enumerating fluorescently labeled cells in 10  $\mu\text{L}$  of blood smears (Fig. 2A). When 10 cells were expected per smear ( $n = 3$  samples), we counted 11, 12, or 13 cells within the range of error for spike-in dilutions at this concentration. The process was linear for the tested 10, 50, and 100 cells per sample ( $R^2 = 0.9529$ ), validating this simple blood smear method. Subsequent comparison of the number of CTC-chip captured cells to CTCs in blood smears revealed an average capture efficiency of 71% with a range from 44% to 125% for 14 mice tested on 6 different days (Fig. 2B).

**Imaging of CTCs using fluorescence, histochemical, and cytokeratin analysis.** Cancer cells captured by the chip were differentiated from mouse leukocytes based on GFP expression using fluorescent microscopy (Fig. 3A). CTCs appeared bright green with a Hoechst-positive nucleus and ranged in size from  $\sim 5 \mu\text{m}$  to  $>20 \mu\text{m}$  in diameter. The cells were observed as both single cells and as clusters (Supplementary Fig. S1). To confirm cells were in fact CTCs, we used an antibody recognizing cytokeratin, an epithelial marker broadly used in pathology labs. Captured CTCs were strongly cytokeratin positive and were easily identified and imaged using bright-field microscopy (Fig. 3B).

**Capture of viable CTCs.** The CTC-chip has been shown to capture live cells from patient blood (9). We wanted to test the ability to both capture live cells and expand them in culture. We therefore used captured cells from mouse P-04 for *ex vivo* growth. The culture was monitored periodically by phase-contrast microscopy. Cells spread out and exhibited a flattened morphology after 1 day in culture. After 5 days, individual colonies of cells were observed. After 12 days in culture, colonies were expanding and cells were growing on top of the posts of the chip. Hoechst 33342

was added to visualize nuclei and propidium iodide was added to identify dead cells. Nearly all cells ( $>99\%$ ) were both GFP positive and nucleated, and very few cells were dead ( $<1\%$ ; Fig. 3C). The cultured cells were also stained with Wright-Giemsa (Fig. 3D) to permit clearer examination of the cellular morphology.

### Validation of transcript panel and CTC collection process.

We evaluated 42 transcripts selected for their relevance in cancer biology (5, 10–12) and abundance in an aliquot of  $\sim 50$  PC-3 cells. Our analysis identified 24 transcripts in our panel that could reliably be measured below a  $Ct$  value of 15 in cultured PC-3 cells and xenograft tumors (Figs. 4 and 5A and B). Adjacent normal mouse tissue did not cross-react with our Taqman assays (data not shown).

Published methods for CTC enrichment do not completely isolate CTCs from blood cells, which can interfere with accurate measurement of transcript levels in CTCs (5). We used LPC to specifically isolate CTCs already greatly enriched by the CTC-chip (9). To examine how the entire CTC collection process affects transcript measurements, we compared fixed tissue culture cells

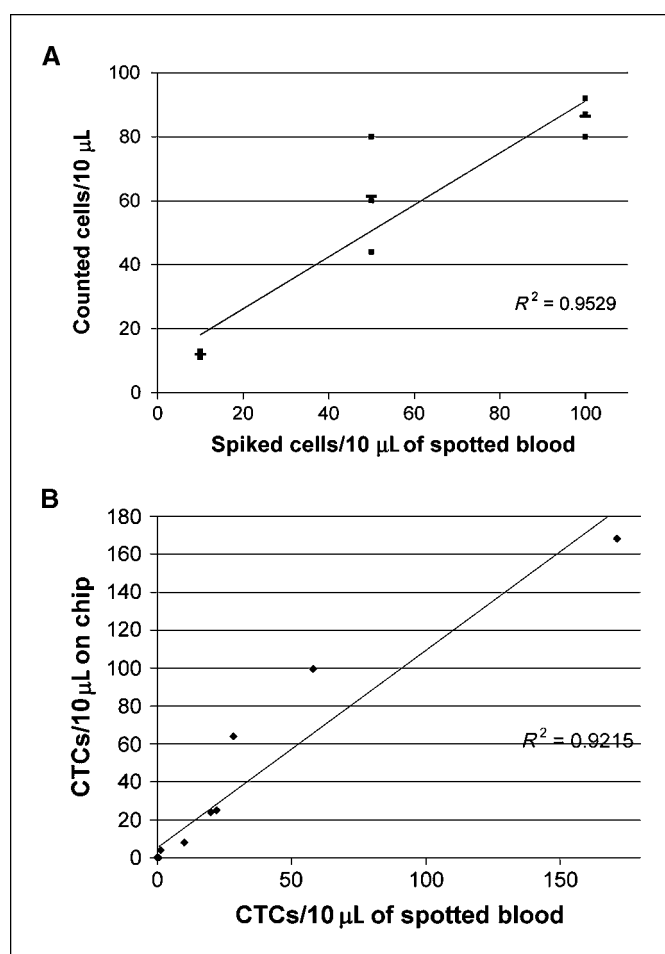
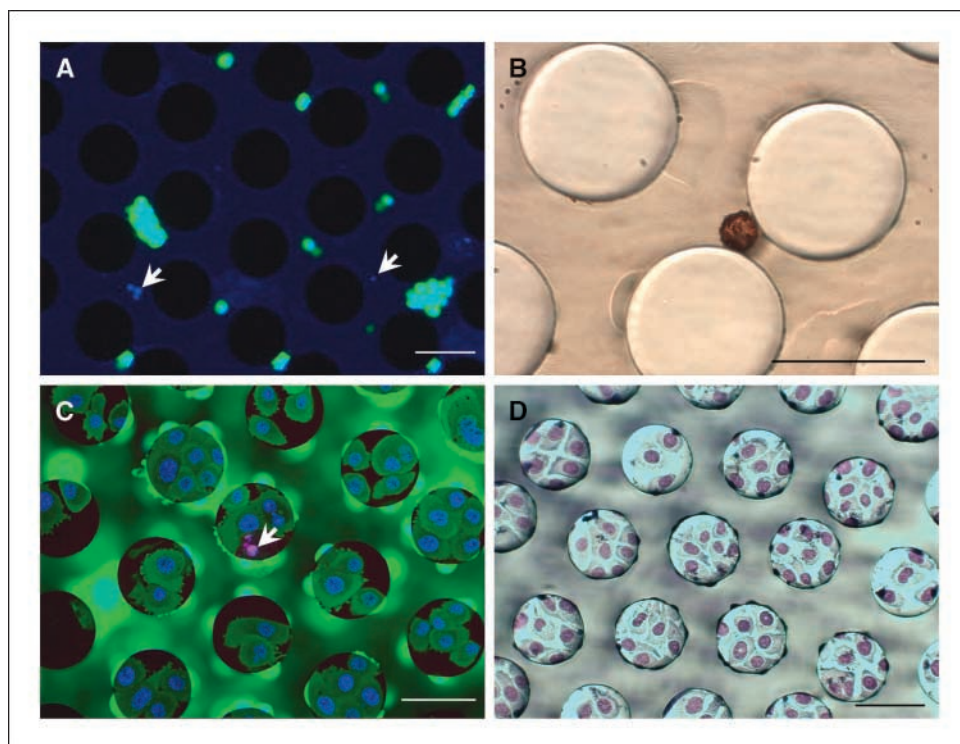


**Figure 2.** Efficiency of enumeration techniques and CTC capture from the PC-3 *in vivo* murine model. *A*, prestained PC-3 cells were titrated into blood to generate 10, 50, and 100 cells per 10  $\mu\text{L}$  aliquot. Cells counted are indicated by squares in the scatter plot. A best-fit line is graphed. The average of the data points is represented by horizontal bars. *B*, counts of GFP<sup>+</sup>/Hoechst<sup>+</sup> cells from 10  $\mu\text{L}$  aliquots of a cardiac bleed compared with counts from 109 to 540  $\mu\text{L}$  of the same bleed run over a CTC-chip. CTC counts were normalized to 10  $\mu\text{L}$ . Thirteen mice are represented in this graph.

**Figure 3.** Imaging of cells on a CTC-chip. **A**, fluorescence imaging of PC-3 CTCs immediately after capture. Cells are stained with Hoechst, and GFP is visible only in CTCs. Mouse leukocytes are smaller and only stain blue. **B**, cytokeratin-stained CTC captured on the chip. **C**, CTCs cultured on the chip after 12 d. Propidium iodide (pink) indicates a dead cell. **D**, Wright-Giemsa staining of cultured CTCs. Scale bars, 100  $\mu$ m.



with fixed cells captured by the CTC-chip and isolated by LPC (Fig. 4). This process decreased the number of evaluable transcripts to 22, which ranged from normalized Ct values of approximately 0 for *GAPDH* to 12 for *CEACAM5*. The correlation between the samples has an  $R^2$  of 0.87 with even greater similarity occurring in transcripts with a normalized Ct below 7. This indicates a dynamic range that extends  $\sim 2$  orders of magnitude below the expression levels of *GAPDH* when  $\sim 50$  cells are measured with this transcription panel.

**Transcriptional analysis of tumor tissue and CTCs.** We next compared transcript levels in primary tumor tissue with those in metastatic tissue collected from the lymph nodes from five mice (Fig. 5A). We found similar gene expression profiles for primary tumor and lymph node metastases, with a best-fit correlation of  $R^2$  of 0.98 for the transcripts analyzed. Moreover, the SD for individual normalized Ct values is low for the group of five mice when either primary tumor or metastatic lymph node tissues are examined. We also collected metastatic tissue from the liver of mouse P-08 and compared transcript levels with those of the primary tumor (Fig. 5B) and again observed high concordance with a best-fit correlation of  $R^2$  of 0.97.

Because we had determined that LPC collection of cells from the CTC-chip retained gene expression profiles, we compared the transcript levels from CTCs isolated from five mice with those from each respective primary tumor. Individual plots from mouse P-08 and P-04 (Fig. 5C and D) show the changes in CTC transcripts relative to the primary tumor. We represented 24 transcript measurements from five mice in a scaled heat map to evaluate the variability (Fig. 6). Within the 2 orders of magnitude dynamic range of the LPC procedure for samples of 50 CTCs, transcripts are strikingly similar across the various mouse tissues and CTCs. *BCL2x* transcripts show differential expression in CTCs relative to malignant tissue.

## Discussion

Many cancer mouse models have been developed in an effort to better recapitulate cancer disease progression. We chose to use the PC-3 xenograft model because it illustrated aspects of the clinical pattern of metastatic spread of advanced clinical prostate cancer (13) and yielded reliably detectable CTCs in pilot experiments. Using a plastic version of the CTC-chip, we showed that fluorescent as well as bright-field analysis was possible. Bright-field analysis enabled the use of LPC to collect CTCs away from contaminating blood cells. Our comparison of a select set of transcripts from primary and metastatic tissues and CTCs shows a strong concordance. We also show culturing of CTCs.

Eliane and colleagues (6) describe a survey of breast cancer models and observed CTC generation in animals injected orthotopically with MDA-MB-231 cells. They serially measured CTCs from the same animal via cardiac punctures to compare tumor progression with CTC generation. We used cardiac bleeds at termination to compare the transcription profile of CTCs with that of tumor material. A less invasive peripheral bleed technique for mice that reliably collects CTCs has not to our knowledge been described. However, the high levels of CTCs collected from the model presented here should support serial bleeds for investigators examining aspects of CTCs with tumor progression.

Using GFP-expressing cells allowed for the monitoring of disease progression by whole-body fluorescent imaging and cells shed from the tumor retained GFP expression allowing unequivocal enumeration. GFP expression is not a prerequisite for CTC imaging. Others have described in detail using fluorescent anti-cytokeratin antibodies to detect CTCs from cancer patients using the CTC-chip (4, 9). We also show that captured cells stain positive for cytokeratin (Fig. 3B) using bright-field immunohistochemical analysis of captured CTCs, a feature made possible by using a plastic CTC-chip. The plastic CTC-chip showed an average recovery efficiency of

71% with CTCs derived from the mouse model, which compares favorably with spike-in studies performed on the silicon CTC-chip (9).

It had previously been shown that CTC numbers do not correlate with the tumor size in a xenograft model (6). Our study confirms this observation. It seems plausible that a trend exists toward increased CTCs with the extent of metastasis as Fig. 1A suggests. Such a trend would normally be difficult to determine due to the difficulty of accurately measuring tumor burden throughout the animal. However, strategies for accurate quantification of tumor metastasis have been published using GFP-positive tumors and could be applied in future studies (14). It is intriguing to think that CTCs are an indicator of metastatic activity. Understanding the etiology of CTCs and the initiation of metastasis may eventually make possible the treatment and control of cancer. Evaluating a possible correlation between metastatic activity and CTC counts is worthy of further investigation to increase our understanding of the biology of CTCs and how they affect disease outcome.

We confirmed that viable CTCs can be captured by the CTC-chip and showed for the first time that the cells could be grown directly on the chip. Because most techniques do not isolate enough CTCs to perform multiple analyses, the possibility that a patient's CTCs can be cultured *ex vivo* and used to characterize the original tumor greatly expands the range of genetic and chemotherapy testing options that otherwise could not be accomplished without a biopsy.

The transcriptional profile of the primary tumor and metastatic tumors from our xenograft model was similar (Figs. 5A and B and 6). This may be explained by the aggressive nature of the model: PC-3 cells were originally isolated from metastatic prostate cancer and may already harbor the corresponding molecular changes necessary for metastatic spread. The fidelity with which the CTC-chip and LPC method maintained the transcript levels of tissue culture cells (Fig. 4) encourages us to believe that the differences observed between transcripts in CTCs compared with primary or metastatic lesions, although modest, are representative of the biological changes that a cell undergoes as it leaves the solid tumor and enters circulation. The methods we describe enable the ability to profile transcripts from patient CTCs. If patient CTCs are also transcriptionally similar to solid tumors, they may be an ideal source of mutational information (4, 9) and a general surrogate for analysis of the primary tumor. Additional comprehensive tests are needed to assess whether this is the case.

When a patient has detectable CTCs, they range widely in abundance (4, 9, 15, 16). In particular, patients with metastatic prostate cancer have been reported to have a mean CTC count of 75 (15). We found that working with 35 to 50 cells (Fig. 4) was sufficient to determine whether the CTC-chip could be used with transcriptional analysis. The mid to low abundance transcripts we examined (e.g., *ERCC1* and *GUS*) require ~30 cells to generate reliable measurements, whereas highly expressed transcripts (e.g., *GAPDH*) can be detected from lower cell inputs (data not shown).

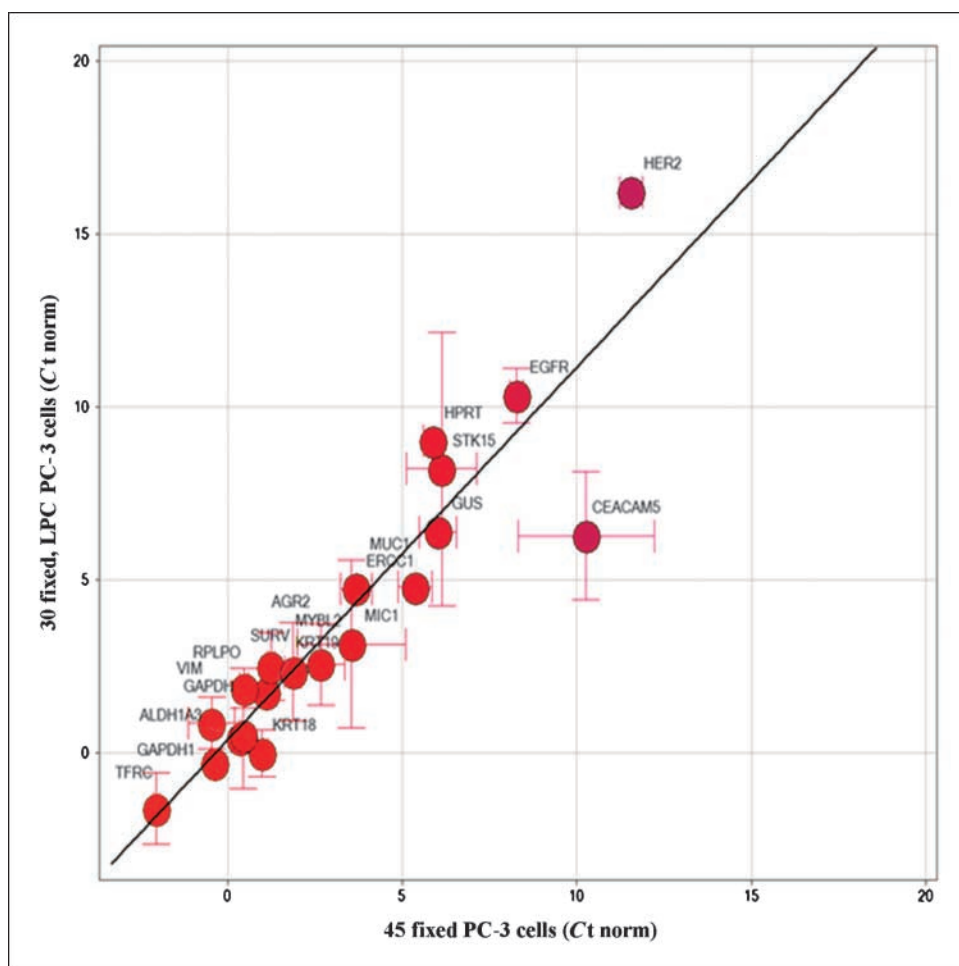


**Figure 4.** PC-3 cells collected by LPC from the CTC-chip are transcriptionally similar to unprocessed PC-3 cells. PC-3 cells were cultured, harvested, and fixed. Duplicate aliquots of ~45 cells were used as templates for molecular analysis. PC-3 cells were also run across the CTC-chip, and 30 cells were collected in duplicate by LPC and used as templates for molecular analysis. All templates were subjected to described transcript analysis, and SD between duplicate RT-PCRs is indicated. Transcripts with Cts of <15 are plotted with a standard curve best-fit line.

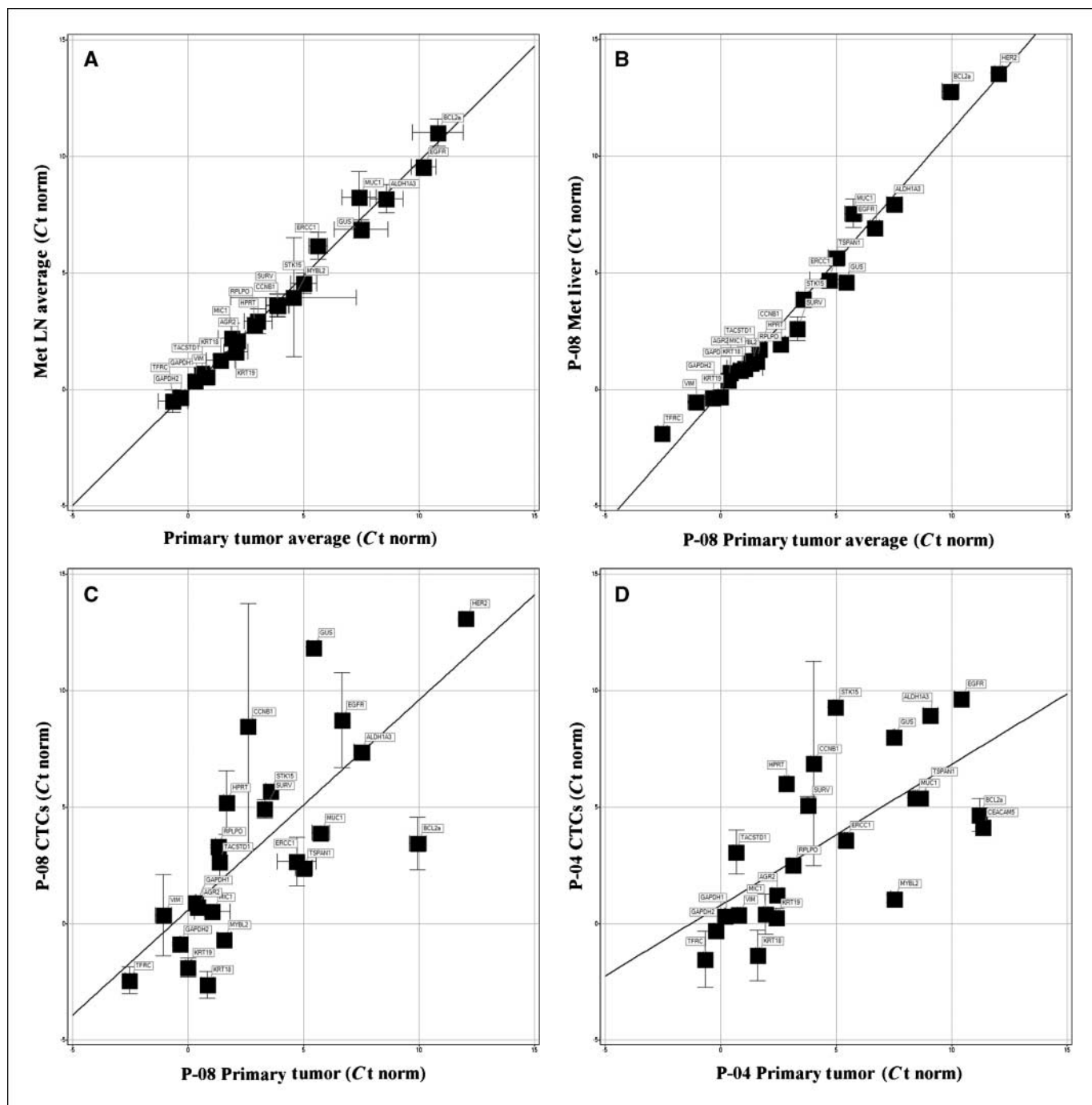


**Figure 5.** Transcript intensities are correlated for primary tumors, metastatic lymph nodes (*Met LN*), metastatic liver (*Met liver*), and CTCs. Tissue RNA (500 pg) and CTCs (50 cells) were subjected to our described RT-PCR preamplification and qPCR. Scatter plots display transcript levels with normalized Cts of <15 and a standard curve best-fit line. Unless otherwise noted, SD corresponds to duplicate RT-PCRs for tissue RNA and triplicate qPCRs for CTCs. *A*, correlation of primary tumors and metastatic lymph nodes as averaged across five experimental mice (P-01, P-03, P-04, P-06, and P-08) with SD across the five listed mice. *B*, transcripts from primary tumor of mouse P-08 compared with metastatic lesions from liver in that mouse. *C* and *D*, transcripts from primary tumor of mouse P-08 ( $R^2 = 0.56$ ) or P-04 ( $R^2 = 0.45$ ), respectively, compared with CTCs.

Because this is within the range of CTCs reportedly isolated from prostate cancer patients, analysis of at least some transcripts from purified patient CTCs is feasible and may provide useful information. Testing the extent to which CTCs are surrogates for the primary biopsy in human patients is under way.

There were some notable changes in transcript abundance. As an example, we observed an increase in the *BCL2 $\alpha$*  gene expression

levels of CTCs relative to primary tumor or metastatic tissue (Figs. 5*C* and *D* and 6). *BCL2 $\alpha$*  is an antiapoptotic gene involved in chemoresistance and is often found up-regulated in cancers (1). Its up-regulation in CTCs may indicate that it is also involved in one of the processes thought to be required for cancer spread, be it escape from the primary tumor, entrance into the bloodstream, or survival on entering circulation. Although following up on this observation

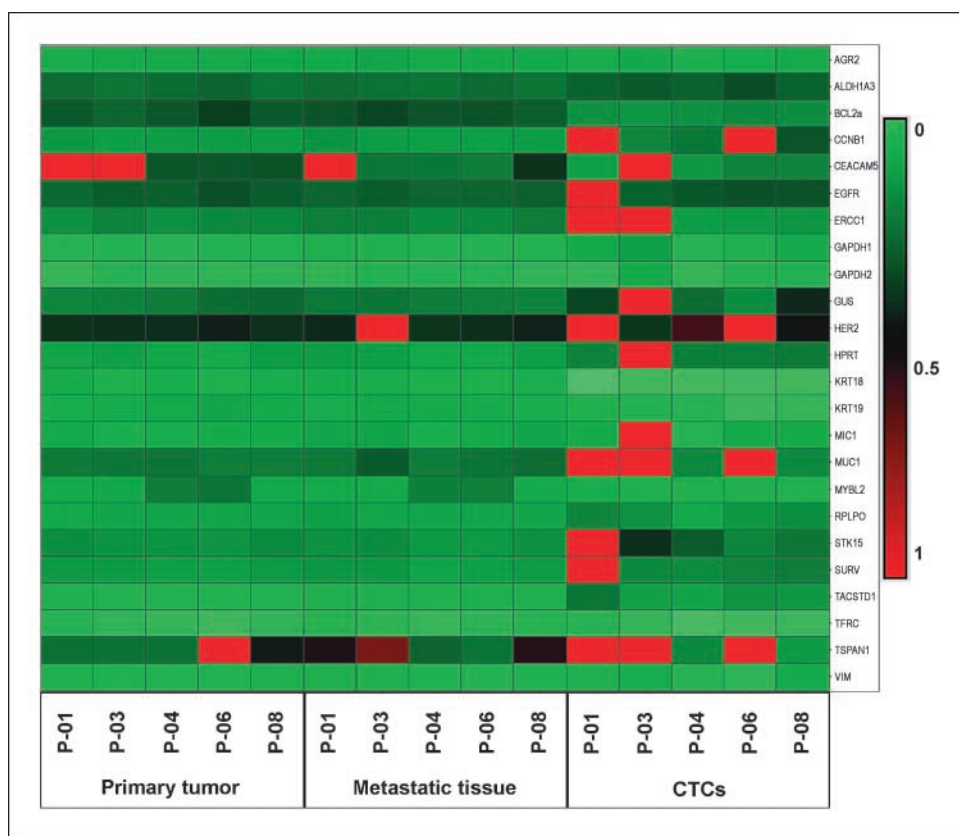


**Figure 6.** LPC of cells enables comparison of purified CTC transcripts with tumor tissues. A heat map was generated by autoscaling each sample to a scale of 0 to 1 (approximate Ct values of 0 to undetectable) for 23 transcripts for five mice to enable intraexperimental comparisons. Samples include primary or metastatic tumor tissue and CTCs as labeled.

is beyond the scope of this work, we believe the system we described is ideally suited for answering such questions.

The shown advantages of the plastic CTC-chip we present include the ability to perform bright-field analysis, including immunohistochemical and Wright-Giemsa staining, and visual monitoring of CTC growth. In addition, the plastic surface enables LPC collection of CTCs away from background cells, which in turn increases the molecular data gathered from CTCs because signal from the background is all but eliminated. Together, this approach greatly expands the information that can be gleaned from fluorescent analysis commonly used in the CTC field. We hope to test the techniques shown here using mice with human samples in the future.

## Disclosure of Potential Conflicts of Interest

No potential conflicts of interest were disclosed.

## Acknowledgments

Received 3/10/09; revised 7/7/09; accepted 7/31/09; published OnlineFirst 9/29/09.

The costs of publication of this article were defrayed in part by the payment of page charges. This article must therefore be hereby marked *advertisement* in accordance with 18 U.S.C. Section 1734 solely to indicate this fact.

We thank the scientists at AntiCancer, Inc. who made recommendations and managed the animals used in this study under contract; Mehmet Toner, Ron Tompkins, and Sunitha Nagrath for sharing their best practices in using the CTC-chip; and all the scientists at CELLective Dx whose efforts laid the foundation for this work.

## References

- Eccles SA, Welch DR. Metastasis: recent discoveries and novel treatment strategies. *Lancet* 2007;369:1742–57.
- Hayes DF, Cristofanilli M, Budd GT, et al. Circulating tumor cells at each follow-up time point during therapy of metastatic breast cancer patients predict progression-free and overall survival. *Clin Cancer Res* 2006;12:4218–24.
- de Bono JS, Scher HI, Montgomery RB, et al. Circulating tumor cells predict survival benefit from treatment in metastatic castration-resistant prostate cancer. *Clin Cancer Res* 2008;14:6302–9.
- Maheswaran S, Sequist LV, Nagrath S, et al. Detection of mutations in EGFR in circulating lung-cancer cells. *N Engl J Med* 2008;359:366–77.
- Smirnov DA, Zweitzig DR, Foulk BW, et al. Global gene expression profiling of circulating tumor cells. *Cancer Res* 2005;65:4993–7.
- Eliane JP, Repollet M, Luker KE, et al. Monitoring serial changes in circulating human breast cancer cells in murine xenograft models. *Cancer Res* 2008;68:5529–32.
- Yang M, Jiang P, Sun FX, et al. A fluorescent orthotopic bone metastasis model of human prostate cancer. *Cancer Res* 1999;59:781–6.
- Glinkii AB, Smith BA, Jiang P, et al. Viable circulating metastatic cells produced in orthotopic but not ectopic prostate cancer models. *Cancer Res* 2003;63:4239–43.
- Nagrath S, Sequist LV, Maheswaran S, et al. Isolation of rare circulating tumour cells in cancer patients by microchip technology. *Nature* 2007;450:1235–9.
- Gupta GP, Nguyen DX, Chiang AC, et al. Mediators of vascular remodelling co-opted for sequential steps in lung metastasis. *Nature* 2007;446:765–70.
- Glinkii GV, Berezovska O, Glinkii AB. Microarray analysis identifies a death-from-cancer signature predicting therapy failure in patients with multiple types of cancer. *J Clin Invest* 2005;115:1503–21.
- Cobleigh MA, Tabesh B, Bitterman P, et al. Tumor gene expression and prognosis in breast cancer patients with 10 or more positive lymph nodes. *Clin Cancer Res* 2005;11:8623–31.
- Fidler IJ. Rationale and methods for the use of nude mice to study the biology and therapy of human cancer metastasis. *Cancer Metastasis Rev* 1986;5:29–49.
- Yang M, Baranov E, Wang JW, et al. Direct external imaging of nascent cancer, tumor progression, angiogenesis, and metastasis on internal organs in the fluorescent orthotopic model. *Proc Natl Acad Sci U S A* 2002;99:3824–9.
- Allard WJ, Matera J, Miller MC, et al. Tumor cells circulate in the peripheral blood of all major carcinomas but not in healthy subjects or patients with nonmalignant diseases. *Clin Cancer Res* 2004;10:6897–904.
- Pachmann K. Longtime recirculating tumor cells in breast cancer patients. *Clin Cancer Res* 2005;11:5657; author reply 5657–8.